



Isner, J. C., Begum, A., Nuehse, T., Hetherington, A. M., & Maathuis, F. J. M. (2018). KIN7 Kinase Regulates the Vacuolar TPK1 K<sup>+</sup> Channel during Stomatal Closure. *Current Biology*, 28(3), 466-472. <https://doi.org/10.1016/j.cub.2017.12.046>

Peer reviewed version

License (if available):  
CC BY-NC-ND

Link to published version (if available):  
[10.1016/j.cub.2017.12.046](https://doi.org/10.1016/j.cub.2017.12.046)

[Link to publication record on the Bristol Research Portal](#)  
PDF-document

This is the author accepted manuscript (AAM). The final published version (version of record) is available online via Elsevier at <https://www.sciencedirect.com/science/article/pii/S0960982217316792> . Please refer to any applicable terms of use of the publisher.

## University of Bristol – Bristol Research Portal

### General rights

This document is made available in accordance with publisher policies. Please cite only the published version using the reference above. Full terms of use are available: <http://www.bristol.ac.uk/red/research-policy/pure/user-guides/brp-terms/>

1

2 KIN7 kinase regulates the vacuolar TPK1 K<sup>+</sup> channel during stomatal  
3 closure.

4  
5 AUTHORS: Jean Charles Isner<sup>1</sup>, Afroza Begum<sup>2</sup>, Thomas Nuehse<sup>3</sup>, Alistair M  
6 Hetherington<sup>1</sup> and Frans J.M. Maathuis<sup>2</sup>

7  
8 Affiliations: <sup>1</sup>) School of Biological Sciences, University of Bristol, Life Sciences Building,  
9 24 Tyndall Avenue, Bristol BS8 1TQ, UK,

10 <sup>2</sup>) Department of Biology, Wentworth Way, University of York, York, YO10 5DD, UK

11 <sup>3</sup>) Faculty of Life Sciences, Michael Smith Building, Oxford Road, Manchester, M13 9PT,  
12 UK

13  
14 Corresponding author and lead contact: Frans J.M. Maathuis, Department of Biology,  
15 University of York, York, YO10 5DD, United Kingdom. Tel: +44-1904-328652, Fax:  
16 +44-1904-328505, email: fjm3@york.ac.uk

## 23 **Summary**

24 Stomata are leaf pores that regulate CO<sub>2</sub> uptake and evapotranspirational water loss. By  
25 controlling CO<sub>2</sub> uptake stomata impact on photosynthesis and dry matter accumulation.  
26 The regulation of evapotranspiration is equally important because it impacts on nutrient  
27 accumulation, leaf cooling and enables the plant to limit water loss during drought [1]. Our  
28 work centres on stomatal closure [2-6]. This involves loss of potassium from the guard cell  
29 by a two-step process. Salt is released across the plasma membrane via anion channels  
30 such as SLAC1 [7-9] and depolarisation-activated channels such as GORK [10,11] with  
31 the net result that cations and anions exit guard cells. However, this critically depends on  
32 K<sup>+</sup> release from the vacuole; With ~160 and 100 mM K<sup>+</sup> in cytoplasm and vacuole of open  
33 guard cells [12], vacuolar K<sup>+</sup> efflux is driven by the negative tonoplast potential and this  
34 expels K<sup>+</sup> from the vacuole via tonoplast K<sup>+</sup> channels like TPK1. In all, guard cell salt  
35 release leads to a loss of turgor that brings about stomatal closure. First we show that the  
36 TPK1 vacuolar K<sup>+</sup> channel is important for ABA and CO<sub>2</sub>-mediated stomatal closure. Next  
37 we reveal that during ABA and CO<sub>2</sub>-mediated closure, TPK1 is phosphorylated and  
38 activated by the KIN7 receptor like protein kinase (RLK) which co-expresses in the  
39 tonoplast and plasma membrane. The net result is K<sup>+</sup> release from the vacuole. Taken  
40 together our work reveals new components involved in guard cell signalling and describes  
41 a new mechanism potentially involved in fine-tuning ABA and CO<sub>2</sub>-induced stomatal  
42 closure.

43

## 44 **Results and Discussion**

45 The tonoplast located channel AtTPK1 [13,14] was previously shown to affect ABA-  
46 induced stomatal closure in *Arabidopsis* [15]. In this investigation we used patch-clamp

47 electrophysiology to show that GC vacuolar preparations exhibited TPK1 activity (Fig. 1A).  
48 Tonoplast channels may show tissue specific properties as was shown for TPC1 [16].  
49 However, single channel conductance and weak voltage dependence of GC TPK1 activity  
50 were the same as previously reported for TPK1 currents from mesophyll cell vacuoles [15].  
51 Addition of 0.5 mM Mg-ATP to the cytoplasmic side of the membrane led to a rapid but  
52 moderate increase in channel activity. Channel activity was further increased when both  
53 Mg-ATP and 14-3-3 protein were present as was shown previously for TPK1 in mesophyll  
54 cells [17,18]. On average, ATP alone caused an increase in channel activity that was  
55 equivalent to an increase in open time (and therefore current) of ~50% whereas ATP+14-  
56 3-3 more than tripled open probability and current (Figure 1B).

57  
58 The S42 residue forms part of the 14-3-3 binding domain in the TPK1 N-terminus and by  
59 using a reconstituted TPK1 N-terminus, Latz, et al. [18] showed that S42 phosphorylation  
60 is required for TPK1-14-3-3 interaction. To test if the same residue is responsible for the  
61 phosphorylation-dependent changes in GC TPK1 activity, we transiently expressed a  
62 mutated (S42A) version of TPK1 in the *tpk1* T-DNA knock out background [15]. The S42A  
63 version mimics a constitutively non-phosphorylated form. Normal currents were recorded  
64 showing that the channel is fully functional (Figure 1A) but the stimulating effects of both  
65 ATP and ATP+14-3-3 were abolished (Figure 1B). Taken together these data show that  
66 in GCs TPK1 shows low basal activity, which increases after phosphorylation at S42 and  
67 is further elevated after binding of 14-3-3. Figure S1 shows that these characteristics were  
68 retained when measuring macroscopic currents.

69

70 *ABA causes phosphorylation of TPK1 in planta*

71 Knowing that ABA induces stomatal closure we decided to test whether TPK1  
72 phosphorylation is ABA-dependent. GC protoplasts were isolated from the *tpk1* mutant  
73 that had been transiently transformed with TPK1::YFP (MW 67.7 kD) and were then  
74 probed with a phosphoserine specific antibody that recognised the phosphorylated 14-3-  
75 3 binding domain [19]. Figure 1C shows a band around 70 kD that increased in intensity  
76 after ABA treatment and was absent in the (non-transformed) *tpk1* null mutant. We also  
77 tested if ABA increased TPK1 phosphorylation in intact tissue; treating leaves with 40  $\mu$ M  
78 ABA for one hour led to increased TPK1 phosphorylation detected in isolated GC  
79 protoplasts (Figure 1D). On the basis of densitometry, 2.5-3-fold higher phosphorylation  
80 signals were recorded after ABA treatment (Figure 1E). These data allow us to conclude  
81 that phosphorylation of TPK1 is regulated by ABA and opens up the possibility that this is  
82 part of the GC ABA signalling network and may be necessary for stomatal closure. It would  
83 be interesting to further test this idea using a phosphomimic TPK1 version, for example  
84 through substitution of S42 with glutamate. Such genotypes could be evaluated for their  
85 transpirational flux, steady state stomatal conductance and responses to various stimuli.

#### 86 *A receptor like kinase is involved in TPK1 phosphorylation*

87 To help identify the protein kinase that was responsible for TPK1 phosphorylation we  
88 interrogated the SUBA database (<http://suba3.plantenergy.uwa.edu.au/>) for protein  
89 kinases that are annotated as tonoplast-localised. A total of 22 kinase isoforms was found  
90 and loss of function mutants were obtained for 16 of these (Table S1). Mutants were tested  
91 for an altered channel 'activation response' to ATP and 14-3-3 (Figures S2A and S2B and  
92 Data S1). The amount of activation generated by ATP varied but was not significantly  
93 different between any of the genotypes (Figure S2B). However, activation by ATP+14-3-3  
94 was significantly ( $p < 0.001$ ) lower in the *kin7* mutant compared to that observed in WT.

95 Furthermore, a role for KIN7 in TPK1 phosphorylation was confirmed by the large  
96 reduction in ABA-induced TPK1 phosphorylation in the *kin7* loss of function mutants  
97 (Figure 1E).

98 KIN7 is ubiquitously expressed in all leaf tissues but to investigate whether KIN7 and TPK1  
99 physically interact at the GC tonoplast we employed a BiFC strategy [20,21]. Figure 2A  
100 shows an intact and an osmotically ruptured GC protoplast co-transformed with TPK1-  
101 YFP<sub>Nt</sub> and TPK1-YFP<sub>Ct</sub>. As expected, fluorescence is clearly localised in the tonoplast.  
102 Similar to the results with TPK1 only, when TPK1-YFP<sub>Ct</sub> was co-transformed with KIN7-  
103 YFP<sub>Nt</sub> there was a prominent fluorescence signal (Figure 2B, bottom left) in many  
104 protoplasts. After osmotic lysis, clear but low intensity fluorescence signal could be  
105 observed in the tonoplast of some cells (Figure 2B, bottom right). In contrast, when TPK1-  
106 YFP<sub>Ct</sub> was co-transformed with KIN8-YFP<sub>Nt</sub> (a kinase very similar to KIN7, see Table S1)  
107 no signal was observed in intact or lysed protoplasts (Figure 2C, n>200). BiFC  
108 experimentation with KIN12, another comparable kinase (Table S1), produced  
109 fluorescence signal but never in the tonoplast (Figure S2, n>200). These results suggest  
110 that TPK1 and KIN7 can directly interact at the tonoplast but that either the incidence is  
111 low (see Figure S2), or alternatively, that relatively few proteins are involved.

112 Apart from electrophysiology and BiFC, we employed a third strategy to probe TPK1-KIN7  
113 interaction. Pull down assays were carried out where the TPK1 N- terminus containing the  
114 14-3-3 domain was used as bait [19] and plant extract derived from shoot tissue  
115 expressing KIN7::YFP as prey. Figure S3 shows that, in addition to the BiFC and the  
116 electrophysiological data, pull down assays too confirm the interaction between TPK1 and  
117 KIN7.

118

119 *kin7 and tpk1 are compromised in ABA and CO<sub>2</sub>-induced stomatal closure*

120 Previously, we showed that in *tpk1* loss of function mutants ABA-induced stomatal closure  
121 is slower than wild type [15]. In the light of our data that TPK1-mediated K<sup>+</sup> release is likely  
122 to depend on KIN7-mediated TPK1 phosphorylation we compared the kinetics of stomatal  
123 closure in wild type, *tpk1* and *kin* loss of function mutants. When ABA-induced stomatal  
124 closure was measured in *tpk1* a reduced closing response was observed (Figure 2D) as  
125 was previously observed [15]. In two independent mutant alleles of *kin7* delayed ABA-  
126 induced closure was also observed. When the *kin7-1* line was rescued with a  
127 35S:*KIN7:YFP* construct, the transformed line reverted to the wildtype phenotype. These  
128 results suggest that TPK1 and KIN7 are part of the GC ABA signalling network. This idea  
129 is supported by the observation that ABA dependent TPK1 phosphorylation was greatly  
130 reduced in both *kin7* mutants (Figure 1E). To investigate whether TPK1 and KIN7 are  
131 involved in other stimuli that cause stomatal closure we exposed the WT, *tpk1* and *kin7*  
132 mutants to elevated levels of CO<sub>2</sub>. Figure 2E shows that *tpk1* and *kin7* mutants are  
133 markedly unresponsive to 1000 ppm CO<sub>2</sub> whether assayed after 3 hours (Figure 2E) or  
134 during continuous conductance measurements (Figure S3). These data suggest that  
135 TPK1 and KIN7 are also involved in the GC CO<sub>2</sub> signalling network.

136 The latter begs the question whether the KIN7-14-3-3-TPK1 pathway also pertains to other  
137 closing stimuli such as the transition from light to dark or a reduction in relative humidity.  
138 Preliminary experiments did not show any drought related phenotype in *tpk1* mutants but,  
139 since the *tpk1* stomatal phenotype primarily affects closing dynamics rather than the  
140 absolute conductance levels [15], more subtle treatments such as alternating relative  
141 humidity may be required. Transition to darkness is another stimulus which so far has not  
142 been investigated in either the *tpk1* or *kin7* genetic background. Future testing of these

143 and other closing stimuli should help determine whether the signalling mechanism we  
144 describe has more general validity.

145

#### 146 *The KIN7 kinase shows dual membrane localisation*

147 As there are reports that KIN7 is localized to the plasma membrane (SUBA:  
148 suba2.plantenergy.uwa.edu.au/) we decided to test whether this protein had a dual  
149 membrane localization in GCs. To test this we used KIN7::YFP fusion proteins which were  
150 stably expressed under control of the 35S promoter or the endogenous KIN7 promoter. In  
151 GC protoplasts derived from transgenic lines, KIN7-YFP was occasionally observed in  
152 both plasma membrane and tonoplast (Figure 3A-F). However, in most cases plasma  
153 membrane signal greatly predominated (Figure 3C and D) to the extent that the tonoplast  
154 signal was only detected after osmotic lysis (Figure 3E and F) when weak but distinct  
155 fluorescence can be distinguished in a proportion of cells as was seen in the BiFC  
156 experiments. This pattern was consistent for KIN7-YFP expression, irrespective of the  
157 promoter driving expression (Figure S4) and clearly point to dual localisation of KIN7. The  
158 latter prompted us to investigate whether KIN7 localisation is sensitive to ABA. One half  
159 of a KIN7-YFP transformed GC population was treated with 40  $\mu$ M ABA and subsequently  
160 the proportion of protoplasts with tonoplast located signal was determined. Figure 3G  
161 shows that the fraction of cells with tonoplast signal more than doubles after exposure to  
162 ABA in a time dependent manner. To independently confirm these findings, we carried out  
163 Western analyses on tonoplast enriched membrane fractions using the tonoplast  
164 aquaporin TIP1;1 as a tonoplast specific marker [22]. Figure 3H shows that initially there  
165 is a minimal KIN7 signal in the lower phase of a two phase partitioned membrane prep.  
166 However, relative to the tonoplast marker TIP1;1, and within 30 min ABA exposure, the



167 KIN7 signal is greatly enhanced, to more than 4-fold the initial value (Figure 3I) while  
168 similar experiments using high CO<sub>2</sub> treatment (1000 ppm, 3h) showed comparable results  
169 with an approximately 3-fold increase towards tonoplast expression (Figure S4). These  
170 results show that ABA may affect TPK1 activity in less than 30 minutes. Cation flux  
171 measurements from *Commelina* epidermal strips [23] show remarkably similar kinetics of  
172 10-20 minutes between ABA addition and cation release. However, these values are  
173 considerably slower than what has been seen for some plasma membrane anion  
174 channels. For example, Levshenko et al [24] recorded anion channel activation 1-2  
175 minutes after ABA exposure. There may be several explanations for this difference; Anion  
176 channel activation is one of the first responses to ABA and may therefore precede slower  
177 cation channel activation. TPK1 activation in intact tissue may be accelerated by unknown  
178 cell wall components or, alternatively, different ABA receptors may be involved in the  
179 coupling to various membranes.

180 The above results show that ABA and CO<sub>2</sub> treatment led to an increase in tonoplast KIN7  
181 signal. The data do not allow to distinguish whether elevated tonoplast expression was  
182 due to *de novo* expression or a consequence of intracellular trafficking. However,  
183 preliminary experiments where tissue was treated with cycloheximide (a protein synthesis  
184 inhibitor) or chlorpromazine (an endocytosis inhibitor) suggest that tonoplast KIN7  
185 expression was not affected by cycloheximide (Figure S4) but sensitive to chlorpromazine.  
186 Such results suggest that endocytosis, rather than *de novo* protein synthesis, is an  
187 essential feature of the shift in KIN7 expression toward the tonoplast.

### 188 *Conclusions*

189 There is a number of conclusions that can be drawn from our work. Our data showing that  
190 TPK1 and KIN7 are involved in CO<sub>2</sub> and ABA is further evidence that both these closure

191 signals are able to access a common set of signalling components whose role it is to bring  
192 about stomatal closure [25]. In addition to identifying that TPK1 activity is regulated by  
193 protein phosphorylation we also report the identity of the regulatory protein kinase. KIN7  
194 has all the hallmarks of an LRR-receptor kinase. It is ubiquitously expressed in many  
195 tissues, including mesophyll cells. In addition to GCs, mesophyll cells have been shown  
196 to respond to ABA, for example by reducing cell volume (e.g. [26]). This opens the  
197 possibility that in mesophyll cells too, KIN7-mediated TPK1 activation plays a role in ABA  
198 signalling. Preliminary patch clamp recordings suggest that KIN7 does impact on TPK1  
199 activity in mesophyll cells which supports the above idea but whether this is linked to  
200 phosphorylation and 14-3-3 binding of mesophyll cell TPK1 remains to be tested.

201 Another major questions to emerge from our work is, what is the link between perception  
202 of ABA and CO<sub>2</sub> on the one hand, and activation of KIN7, binding of 14-3-3 and activation  
203 of TPK1 on the other? Upstream signalling components could include well known players  
204 such as ABI and OST gene products. Further experimentation with ABA signalling  
205 mutants, or ones in CO<sub>2</sub> signalling components such as HT1 kinase, RHC1 and RBOH-  
206 D/F, will help reveal such interactors. Downstream, 14-3-3 must bring about a  
207 conformational change that greatly stimulates channel opening. One mechanism suggests  
208 that the TPK1 gate is directly controlled via Ca<sup>2+</sup> binding to C-terminal EF domains [27]  
209 and a model where 14-3-3 sensitises TPK1 Ca<sup>2+</sup> dependence not only provides a  
210 mechanistic explanation but could be tested using electrophysiology.

211 It is noteworthy that ABA treatment has been reported to result in KIN7 phosphorylation at  
212 its C-terminus [28]. If the phosphorylation results in alterations to KIN7 activity this would  
213 suggest that at least one additional protein kinase is involved in this signalling network.

214 Our data showing that KIN7 is localized at both the plasma and tonoplast membranes is

215 supportive of a dynamic, stimulus-induced, mechanism of TPK1 regulation. Inhibition by  
216 the endocytotic inhibitor chlorpromazine of the relative shift toward tonoplast expression  
217 of KIN7 suggests that the observed increase in KIN7 tonoplast localisation does not  
218 originate from de novo KIN7 biosynthesis, but occurs via a hitherto uncharacterised  
219 trafficking pathway. Although such findings can only be preliminary and will need further  
220 support, retrograde endocytotic trafficking of plasma membrane proteins to  
221 endocompartments has been reported: In animals compartmentalisation of receptor  
222 kinases generates endosome specific signal transduction complexes [29]. In plants too,  
223 trafficking of the steroid receptor kinase BRI1 to endosomal vesicles is believed to be  
224 important in intracellular signalling [30].

225 Control of TPK1 activity through the stimulus-induced localization of KIN7, be it via  
226 modulation of expression or via trafficking, represents an attractive mechanism for exerting  
227 control over  $K^+$  efflux from vacuoles. We have summarised what we know about this  
228 pathway in the schema described in Figure 4. What might be the function of this form of  
229 regulation? Our phenotypic data showing that mutants in this pathway are distinguished  
230 by exhibiting slower rates of closure suggest that this pathway might be in the fine-tuning  
231 of stomatal responses rather than switching closure on (or off). However, a better  
232 understanding awaits the discovery of additional components in the network.

233 **ACKNOWLEDGEMENTS:** We thank Bert de Boer (Vrije Universiteit Amsterdam) for his  
234 kind gift of 14-3-3 protein and Ingo Dreyer (Universidad de Talca, Chile) for his kind gift of  
235 BiFC vectors. We thank Wioletta Pijacka (University of Bristol, UK) for her technical help  
236 with Western blotting. AMH and J-C I wish to acknowledge grant support from the UK  
237 BBSRC (BB/J002364/1) and the Leverhulme Trust.

238 **AUTHOR CONTRIBUTIONS:**

239 JCI and FJM designed research; JCI, FJM, AB and TSN performed research; JCI and  
240 FJM analysed data; FJM, AMH and JCI wrote the paper.

## 241 **DECLARATION OF INTERESTS**

242 The authors declare no competing interests.

## 243 **REFERENCES**

- 244 1. Hetherington, A.M., and Woodward, F.I. (2003). The role of stomata in sensing and driving  
245 environmental change. *Nature*. *424*, 901-908.
- 246 2. Roelfsema, M.R., Levchenko, V., and Hedrich, R. (2004). ABA depolarizes guard cells in  
247 intact plants, through a transient activation of R- and S-type anion channels. *Plant J.* *37*, 578-588.
- 248 3. Schroeder, J., Gethyn J Allen, Veronique Hugouvieux, June M Kwak, a., and Waner, D.  
249 (2001). Guard cell signal transduction. *Annu Rev Plant Physiol Plant Mol Biol.* *52*, 627-658.
- 250 4. Assmann, S.M., and Jegla, T. (2016) Guard cell sensory systems: recent insights on stomatal  
251 responses to light, ABA and CO<sub>2</sub>. *Curr Opin Plant Biology* *33*, 157-167.
- 252 5. Raghavendra, A.S., Gonugunta, V.K., Christmann, A., and Grill, E. (2010) ABA perception  
253 and signalling. *Trends in Plant Sciences* *15*, 395-401.
- 254 6. Munemasa, S., Hauser, F., Park, J., Waadt, R., Brandt, B., and Schroeder, J.I. (2015)  
255 Mechanisms of ABA-mediated control of stomatal aperture. *Current Opinion in Plant Biology* *28*,  
256 154-162.
- 257 7. Geiger, D., Maierhofer, T., AL-Rasheid, K.A.S., Scherzer, S., Mumm, P., Liese, A., Ache,  
258 P., Wellmann, C., Marten, I., Grill, E., et al. (2011). Stomatal closure by fast abscisic acid signaling  
259 is mediated by the guard cell anion channel SLAH3 and the receptor RCAR1. *Sci Signal.* *4*, ra32.
- 260 8. Geiger, D., Scherzer, S., Mumm, P., Stange, A., Marten, I., Bauer, H., Ache, P., Matschi,  
261 S., Liese, A., Al-Rasheid, K.A.S., et al. (2009). Activity of guard cell anion channel SLAC1 is  
262 controlled by drought-stress signaling kinase-phosphatase pair. *Proc Natl Acad Sci USA.* *106*,  
263 21425-21430.
- 264 9. Imes, D., Mumm, P., Bohm, J., Al-Rasheid, K.A., Marten, I., Geiger, D., and Hedrich, R.  
265 (2013). Open stomata 1 (OST1) kinase controls R-type anion channel QUAC1 in *Arabidopsis* guard  
266 cells. *Plant J.* *74*, 372-382.
- 267 10. Ache, P., Becker, D., Ivashikina, N., Dietrich, P., Roelfsema, M.R., Hedrich, R. (2000).  
268 GORK, a delayed outward rectifier expressed in guard cells of *Arabidopsis thaliana*, is a K(+)-  
269 selective, K(+)-sensing ion channel. *FEBS Lett.* *486*, 93-98.
- 270 11. Hosy, E., Vavasseur, A., Mouline, K., Dreyer, I., Gaymard, F., Porée, F., Boucherez, J.,  
271 Lebaudy, A., Bouchez, D., Véry, A.-A., et al. (2003). The *Arabidopsis* outward K<sup>+</sup> channel GORK  
272 is involved in regulation of stomatal movements and plant transpiration. *Proc Natl Acad Sci USA.*  
273 *100*, 5549-5554.
- 274 12. Hills, A., Chen, Z.H., Amtmann, A., Blatt, M.R., Lew, V.L. (2012). OnGuard, a  
275 Computational Platform for Quantitative Kinetic Modeling of Guard Cell Physiology. *Plant*  
276 *Physiol.* *159*(3):1026-42.
- 277 13. Dunkel, M., Latz, A., Schumacher, K., Muller, T., Becker, D., and Hedrich, R. (2008).  
278 Targeting of vacuolar membrane localized members of the TPK channel family. *Mol Plant.* *1*, 938-  
279 949.

- 280 14. Voelker, C., Gomez-Porras, J.L., Becker, D., Hamamoto, S., Uozumi, N., Gambale, F.,  
281 Mueller-Roeber, B., Czempinski, K., and Dreyer, I. (2010). Roles of tandem-pore K<sup>+</sup> channels in  
282 plants - a puzzle still to be solved. *Plant Biol* 12 *Suppl* 1, 56-63.
- 283 15. Gobert, A., Isayenkov, S., Voelker, C., Czempinski, K., and Maathuis, F.J. (2007). The two-  
284 pore channel TPK1 gene encodes the vacuolar K<sup>+</sup> conductance and plays a role in K<sup>+</sup> homeostasis.  
285 *Proc Natl Acad Sci USA*. 104, 10726-10731.
- 286 16. Rienmüller, F., Beyhl, D., Lautner, S., Fromm, J., Al-Rasheid, K.A., Ache, P., Farmer, E.E.,  
287 Marten, I., Hedrich, R. (2010) Guard cell-specific calcium sensitivity of high density and activity  
288 SV/TPC1 channels. *Plant Cell Physiol*. 51, 1548-54.
- 289 17. Isayenkov, S., Isner, J.C., and Maathuis, F.J. (2011). Rice two-pore K<sup>+</sup> channels are  
290 expressed in different types of vacuoles. *Plant Cell*. 23, 756-768.
- 291 18. Latz, A., Becker, D., Hekman, M., Muller, T., Beyhl, D., Marten, I., Eing, C., Fischer, A.,  
292 Dunkel, M., Bertl, A., et al. (2007). TPK1, a Ca<sup>2+</sup>-regulated *Arabidopsis* vacuole two-pore K<sup>+</sup>  
293 channel is activated by 14-3-3 proteins. *Plant J*. 52, 449-459.
- 294 19. Latz, A., Mehlmer, N., Zapf, S., Mueller, T.D., Wurzinger, B., Pfister, B., Csaszar, E.,  
295 Hedrich, R., Teige, M., and Becker, D. (2013). Salt stress triggers phosphorylation of the  
296 *Arabidopsis* vacuolar K<sup>+</sup> channel TPK1 by calcium-dependent protein kinases (CDPKs). *Mol Plant*.  
297 6, 1274-1289.
- 298 20. Waadt, R., Schmidt, L.K., Lohse, M., Hashimoto, K., Bock, R., and Kudla, J. (2008).  
299 Multicolor bimolecular fluorescence complementation reveals simultaneous formation of  
300 alternative CBL/CIPK complexes in planta. *Plant J*. 56, 505-516.
- 301 21. Kudla, J., and Bock, R. (2016). Lighting the way to protein-protein interactions:  
302 Recommendations on best practices for bimolecular fluorescence complementation analyses. *Plant*  
303 *Cell*. 28, 1002-1008.
- 304 22. Ludevid, D., Hofte, H., Himelblau, E., and Chrispeels, M.J. (1992). The expression pattern  
305 of the tonoplast intrinsic protein gamma-tip in *Arabidopsis thaliana* is correlated with cell  
306 enlargement. *Plant Physiol*. 100, 1633-1639.
- 307 23. MacRobbie EA (2006) Control of volume and turgor in stomatal guard cells. *J Membr Biol*  
308 210: 131-42
- 309 24. Levchenko, V., Konrad, K.R., Dietrich, P., Roelfsema, M.R., Hedrich, R.(2005). Cytosolic  
310 abscisic acid activates guard cell anion channels without preceding Ca<sup>2+</sup> signals. *Proc Natl Acad*  
311 *Sci U S A*. 15;102(11):4203-8.
- 312 25. Chater, C., Peng, K., Movahedi, M., Dunn, Jessica A., Walker, Heather J., Liang, Y.-K.,  
313 McLachlan, Deirdre H., Casson, S., Isner, Jean C., Wilson, I., et al. Elevated CO<sub>2</sub>-induced  
314 responses in stomata require ABA and ABA signaling. *Curr Biol*. 25, 2709-2716.
- 315 26. Kolla, V.A., Suhita, D., Raghavendra, A.S. (2004) Marked changes in volume of mesophyll  
316 protoplasts of pea (*Pisum sativum*) on exposure to growth hormones. *J Plant Physiol*. 161, 557-562.
- 317 27. Hartley, T.N., Maathuis, F.J.M. (2015) Allelic variation in the vacuolar TPK1 channel  
318 affects its calcium dependence. *FEBS Lett*. 590, 110-117.
- 319 28. Chen, Y., Hoehenwarter, W., and Weckwerth, W. (2010). Comparative analysis of  
320 phytohormone-responsive phosphoproteins in *Arabidopsis thaliana* using TiO<sub>2</sub>-phosphopeptide  
321 enrichment and mass accuracy precursor alignment. *Plant J*. 63, 1-17.
- 322 29. Villaseñor, R., Nonaka, H., Del Conte-Zerial, P., Kalaidzidis, Y., and Zerial, M. (2015).  
323 Regulation of EGFR signal transduction by analogue-to-digital conversion in endosomes. *eLife*. 4,  
324 e06156.
- 325 30. Geldner, N., and Robatzek, S. (2008). Plant receptors go endosomal: a moving view on  
326 signal transduction. *Plant Physiol*. 147, 1565-1574.

- 327 31. Schindelin, J., Rueden, C.T., Hiner, M.C., and Eliceiri, K.W. (2015). The ImageJ  
328 ecosystem: An open platform for biomedical image analysis. *Mol Reprod Dev.* 82, 518-529.
- 329 32. Pijacka, W., Clifford, B., Tilburgs, C., Joles, J.A., Langley-Evans, S., and McMullen, S.  
330 (2015). Protective role of female gender in programmed accelerated renal aging in the rat. *Physiol*  
331 *Rep.* 3.
- 332 33. Hellens, R., Edwards, E.A., Leyland, N., Bean, S., and Mullineaux, P. (2000). pGreen: a  
333 versatile and flexible binary Ti vector for *Agrobacterium*-mediated plant transformation. *Plant Mol*  
334 *Biol.* 42, 819-832.
- 335 34. Pandey, S., Wang, X.Q., Coursol, S.A., and Assmann, S.M. (2002). Preparation and  
336 applications of *Arabidopsis thaliana* guard cell protoplasts. *New Phytol.* 153, 517-526.
- 337 35. Maathuis, F.J.M., May, S.T., Graham, N.S., Bowen, H.C., Jelitto, T.C., Trimmer, P.,  
338 Bennett, M.J., Sanders, D., and White, P.J. (1998). Cell marking in *Arabidopsis thaliana* and its  
339 application to patch-clamp studies. *Plant J.* 15, 843-851.
- 340 36. Sinnige, M.P., Roobeek, I., Bunney, T.D., Visser, A.J., Mol, J.N., and de Boer, A.H. (2005).  
341 Single amino acid variation in barley 14-3-3 proteins leads to functional isoform specificity in the  
342 regulation of nitrate reductase. *Plant J.* 44, 1001-1009.
- 343 37. Lund, A., and Fuglsang, A.T. (2012). Purification of plant plasma membranes by two-phase  
344 partitioning and measurement of H<sup>+</sup> pumping. *Methods Mol Biol.* 913, 217-223.
- 345 38. Rea, P.A., Britten, C.J., and Sarafian, V. (1992). Common identity of substrate binding  
346 subunit of vacuolar H<sup>+</sup>-translocating inorganic pyrophosphatase of higher plant cells. *Plant Physiol.*  
347 *100*, 723-732.
- 348

349 **Figure legends:**

350 **Figure 1: GC TPK1 currents and ABA induced TPK1 phosphorylation.**

351 **(A)** Representative TPK1 currents from one cytoplasmic side out excised patch shows  
352 TPK1 currents in control buffer, after addition of MgATP (0.5 mM) or MgATP plus 14-3-  
353 3 (100 nM). Mutation of the N-terminal serine 42 to alanine (S42A) leaves channel  
354 activity intact but abrogates the effect of ATP and 14-3-3. Currents were recorded at -  
355 40 mV and left side arrows indicate closed levels. Amplitude histograms on right show  
356 increase in channel openings for wildtype but not S42A. 'Po' open probability  
357 quantification based on 60 sec records. **(B)** Normalised relative channel activity, based  
358 on open probability data obtained at -80 mV, showing ATP stimulates activity by around  
359 45% and ATP plus 14-3-3 stimulates activity by over 300%, while no significant effect of  
360 ATP+14-3-3 is observed for the S42A mutant protein (n=3 independent membrane

361 patches for each condition, error bars are standard errors.) Data were analysed using  
362 one way ANOVA with Tukey post-hoc analysis comparison with control conditions,  
363 asterisks denoting  $p < 0.05$ . **(C)** GCs from *tpk1* plants were isolated and transiently  
364 transformed with TPK1-YFP. Approx 12-16h after transformation half the protoplasts  
365 were treated with ABA (1h, 40  $\mu$ M). Right hand panel: non transformed (NT) protoplasts  
366 show complete absence of signal ('T' are transformed protoplasts from the same prep).  
367 **(D)** Guard cells isolated from ABA-treated *tpk1* loss of function plants, control leaves  
368 (WT plants) or ABA treated leaves (WT plants). In (C) and (D), top panels show typical  
369 example of blots with antibody against the phosphorylated TPK1 N-terminus. Bottom  
370 panels show total protein staining. **(E)** Densitometry based (n=3, bars denote standard  
371 errors) fold-changes in TPK1 phosphorylation in control (WT-con) and ABA treated  
372 (WT\_ABA\_L) leaves or protoplasts (WT\_ABA\_P) and in null mutants of the LRR kinase  
373 KIN7 (*kin7\_ABA*). Data were analysed using one way ANOVA with Tukey post-hoc  
374 analysis comparison with control conditions, asterisks denoting  $p < 0.05$ . (See also  
375 Figures S1 and Table S1).

376 **Figure 2: Bimolecular fluorescence complementation and loss of function**  
377 **phenotypes in *tpk1* and *kin7*.**

378 **(A)** Representative image for Arabidopsis GCs cotransformed with TPK1<sub>YFP-Nt</sub> plus  
379 TPK1<sub>YFP-Ct</sub>. Note clear vacuolar fluorescence. **(B)** GC protoplasts expressing KIN7<sub>YFP-</sub>  
380 <sub>Nt</sub> plus TPK1<sub>YFP-Ct</sub>. Note clear signal in the tonoplast. **(C)** GC protoplast expressing  
381 KIN8<sub>YFP-Nt</sub> plus TPK1<sub>YFP-Ct</sub>. Note the absence of any fluorescence signal. In all cases,  
382 top two panels show DIG images of intact and osmotically ruptured protoplast (releasing  
383 the large central vacuole). Bottom panels show corresponding YFP fluorescence signal.  
384 Scale bar is 5  $\mu$ m. **(D)** Leaves of wild type (WT), TPK1 and KIN7 loss of function mutants

385 KIN7 complemented plants were exposed to 100, 10 or 1  $\mu$ M ABA and start ('Control')  
386 and end (30 minute ABA exposure) conductance values were recorded. **(E)** Stomata  
387 were opened by exposure of leaves to 400 ppm CO<sub>2</sub> for 2 hours. Subsequently, peels  
388 were either aerated with 1000 ppm [CO<sub>2</sub>] or continued to be aerated with 400 ppm [CO<sub>2</sub>].  
389 Three hours later, stomatal apertures were measured. Data in D and E were analysed  
390 for significance using a one way ANOVA with Tukey post-hoc analysis. Asterisk denotes  
391  $p < 0.05$ . (See also Figures S2 and S3).

392 **Figure 3: KIN7:YFP expression patterns.**

393 **(A)** DIC image of intact Arabidopsis GC transformed with KIN7:YFP. **(B)** Corresponding  
394 fluorescence image showing expression in both plasma membrane and tonoplast  
395 (arrows). **(C and D)** DIC and fluorescence image of GC protoplast showing prominent  
396 expression in the plasma membrane only. **(E)** DIC image of osmotically ruptured  
397 protoplast releasing the large vacuole. **(F)** Corresponding fluorescence image showing  
398 weak but distinct tonoplast expression. **(G)** The proportion of lysed guard cell  
399 protoplasts that shows tonoplast KIN7 expression increases after ABA treatment. **(H)**  
400 Western immunoblot showing increasing level of KIN7-GFP expression in response to  
401 ABA. The vacuole specific aquaporin TIP1;1 was used as tonoplast marker whereas the  
402 lack of cross reactivity with the H<sup>+</sup>-ATPase AHA1 (a plasma membrane specific marker)  
403 in the 'lower phase' (LP) shows absence of plasma membrane. 'MF': microsomal  
404 fraction showing positive reactivity for all three probes. **(I)** Quantification based on  
405 densitometry measurements (using ImageJ) of relative increase in KIN7 expression in  
406 the tonoplast. Scale bar in A-F is 7  $\mu$ m. Data depicted in G and I are based on 3 or more  
407 independent experiments, bars denote standard errors and data were analysed using



408 one way ANOVA with Tukey post-hoc analysis comparison with control conditions.

409 Asterisk denotes  $p < 0.05$ . (See also Figure S4).

410 **Figure 4: A model for coupling ABA and TPK1.**

411 ABA perception leads to activation of the LRR kinase KIN7. Increased tonoplast

412 expression of KIN7 and/or KIN7 traffic from plasma membrane (PM) to tonoplast (TO)

413 brings KIN7 in the vicinity of TPK1. At the tonoplast, phosphorylation of S42 in the N-

414 terminal 14-3-3 binding domain allows 14-3-3 binding to TPK1, which leads to drastically

415 increased TPK1 activity and stomatal closure.

416 **METHODS**

417 **CONTACT FOR REAGENT AND RESOURCE SHARING**

418 Further information and requests for resources and reagents should be directed to and

419 will be fulfilled by the Lead Contact, Frans Maathuis (frans.maathuis@york.ac.uk)

420 **EXPERIMENTAL MODEL AND SUBJECT DETAILS**

421 **Plant material and growth.** *Arabidopsis thaliana* (L) ecotype Columbia (0) wild type,

422 *tpk1* (SALK line 146903; [15] and kinase mutants and kinase mutants obtained from

423 NASC (see Table S1).

424 **METHOD DETAILS**

425 **Plants**

426 *Arabidopsis thaliana* (L) ecotype Columbia (0) wild type, *tpk1* and kinase mutants were grown for

427 3 to 4 weeks in soil (F2, Levington, UK) at 18/22°C night/day temperature in a glasshouse with day

428 lengths of 14 h, supplemented with artificial light of around  $200 \mu\text{mol m}^{-2} \text{sec}^{-1}$  as described [17].

429 T-DNA insertion lines for kinase mutants and the forward and reverse primers that were used to test

430 for homozygosity and transcript can be found in Table S1 and S2.

431 **Cloning of kinases in the BiFC vector**

432 KIN8 and KIN12 were cloned from cDNA produced from total RNA: Total RNA was extracted

433 from *Arabidopsis* leaves with RNeasy Plant Mini Kit (Qiagen GmbH, Germany). First strand cDNA

434 was synthesised using SuperScript II Reverse Transcriptase kit (Life Technologies Ltd, UK) with  
435 the following primers: kin8bifc fwd and kin8bifc rev, kin12bifc fwd and kin12bifc rev (Table S2).  
436 KIN8 and KIN12 fragments were amplified using kin8bifc fwd+kin8bifc rev and kin12bifc fwd+  
437 kin12bifc rev primers respectively (Table S2). KIN7 was PCR-amplified from the full length cDNA  
438 clone U12357 (<http://abrc.osu.edu/>) using the kin7bifc fwd and kin7bifc rev primers (Table S2).  
439 Amplified fragments were digested using SpeI and XhoI for KIN7 and KIN8 or BamHI and XhoI  
440 for KIN12 and inserted in pSPYNE [20].

#### 441 **Quantification of BiFC signals**

442 To be able to compare BiFC signals from various combinations, ImageJ software [31]) was used to  
443 measure signal intensity from the vacuolar and plasma membranes. Values were corrected by  
444 subtracting signal intensity from nearby background. Signal from TPK1\_YFP\_Nt+TPK1\_YFP\_Ct  
445 (which forms a dimer) was used as positive control and the signal from  
446 kin12\_YFP\_Nt+TPK1\_YFP\_Ct (which shows signal in ER and PM but not, or extremely little, in  
447 the tonoplast) used as negative control. Quantitative data for BiFC fluorescence signal are shown in  
448 Figure S2.

#### 449 **TPK1 pull-down assay**

450 Pull-down assays were used to confirm the interaction between the N-terminus part of TPK1 and  
451 KIN7. The sequence corresponding to the first 81 amino acids of TPK1 (NTPK1) was amplified by  
452 PCR using tpk1bamhI and tpk1xhoI primers (Table S2) and cloned into the pGEX6P-1 vector  
453 (GE Healthcare, Amersham, UK). GST and GST::NTPK1 expression was induced in 1l culture of  
454 *E. coli* BL21 at 37°C with 1mM IPTG for 4 hours. Cells were collected and lysed in PBS-T buffer  
455 (PBS pH 7.3, 0.1% Trion X-100) by sonication. After centrifugation, the lysate was cleared using  
456 0.45 µm filters. GST or GST::NTPK1 was bound to 500 µl of Glutathione Sepharose 4B (GE  
457 Healthcare, Amersham, UK) for 2h. 50 µl bead aliquots washed with buffer P (HEPES 50mM  
458 pH7.3, 2mM CaCl<sub>2</sub>, 2mM MgCl<sub>2</sub>, 2mM KCl, 100mM NaCl, 1% CHAPS) and protease inhibitor  
459 cocktail IV (Calbiochem, Merck, Feltham, UK) were incubated overnight with either proteins  
460 extracted with buffer P from plants expressing wild type KIN7 or KIN7::YFP. The next day, beads  
461 were washed 4 times with the same buffer. Bound proteins were eluted with SDS-PAGE Protein  
462 Sample Buffer (2×) and loaded on a 10% acrylamide gel. Western blotting was performed as  
463 described previously [32]. Rabbit anti-GFP (Thermofisher, Paisley, UK) and swine anti-rabbit  
464 Immunoglobulins HRP (Agilent, Stockport, UK) were used and the resulting signal in the presence

465 of Luminata Forte substrate (Merck, Feltham, UK) was imaged with Fusion Pulse imaging system  
466 (Vilber Lourmat, Marne-la-Vallée, France).

#### 467 **Cloning of KIN7:YFP and Arabidopsis plant transformation**

468 KIN7 was PCR amplified from the clone U12357 (<http://abrc.osu.edu/>) with the kin7yfpfwd and  
469 kin7yfprev primers (Table S2) and inserted in the pART7 vector [33]. The NotI fragment containing  
470 the 35S:KIN7:YFP fragment was subsequently inserted in pGREEN0229. *Arabidopsis* plants were  
471 transformed by floral spraying as described in [33]. Briefly, *Agrobacterium* was grown in 50 mL  
472 liquid YEB medium for two days or until the OD reached 3. The cells were spun down (5 min,  
473 4000g) and resuspended in 20 mL of 0.1x MS medium, 5% sugar, 0.1% Silwet L-77, pH 5.7. Every  
474 two weeks, flowering plants were sprayed with *Agrobacterium* using an airbrush. For  
475 pKin7::KIN7:YFP, 589bp upstream of the ATG was amplified from genomic DNA with  
476 promkin7fwd and promkin7rev primer (Table S2). This Fragment was inserted in the  
477 35S::KIN7::YFP vector instead of the 35S promoter, which was removed using StuI and XhoI.

#### 478 **Protoplast isolation:**

479 Guard cell protoplasts were isolated as described by Pandey, et al. [34]. 40 fully expanded leaves  
480 were blended in water for 1 minute using a waring SS515 Blender (Cole-Parmer UK) and poured  
481 onto a 200 µm mesh to collect epidermes. Epidermes were incubated in 45% H<sub>2</sub>O, 55% basic  
482 solution (0.5 mM CaCl<sub>2</sub>, 0.5mM MgCl<sub>2</sub>, 0.01 mM KH<sub>2</sub>PO<sub>4</sub>, 0.5 mM ascorbic acid, 550 mM  
483 sorbitol, 0.2% BSA, 0.7% cellulysin, 5 mM MES/Tris pH 5.5) for 1.5 h at 30°C. The epidermes  
484 were then incubated in basic solution supplemented with cellulase Onozuka RS 0.01% and  
485 pectolyase Y23 for 1 h at 30°C. Guard cell protoplasts were collected after passing the solution  
486 through a 20 µm mesh.

487 Mesophyll protoplast were extracted from Arabidopsis leaves according to {Isayenkov, 2011 #4}.  
488 Leaves were cut in 1-mm sections and digested for 4 h in an enzyme solution containing 1.5%  
489 cellulose RS, 0.75% macerozyme, 0.6 m mannitol, 10 mM 2-(N-morpholine)-ethanesulphonic acid  
490 (MES), pH 5.6 and 1 mM CaCl<sub>2</sub>, in which proteases were heat inactivated for 10 min at 55°C.  
491 Protoplasts were filtered and centrifuged for 3 min at 500 g and resuspended in protoplast incubation  
492 solution (0.6 M mannitol, 4 mM MES, pH 5.7, 4 mM KCl and 3 mM CaCl<sub>2</sub>)

#### 493 **Electrophysiology**

494 Vacuole release, equipment and analyses were as described in Maathuis, et al. [35]. After transfer  
495 of protoplasts to the recording chamber, vacuoles were released by washing protoplasts with a

496 solution containing 10 mM EDTA, 10 mM EGTA, pH 8 with an osmolarity of 350 mOsm. Standard  
497 experimental solutions for bath and pipette contained 100 mM KCl, 0.1 mM CaCl<sub>2</sub>, 5 mM MES/Tris  
498 pH 7 and sorbitol adjusted to 430 mOsm total osmolarity. Open probability (Po) was calculated as  
499 described in Gobert, et al. [15] and defined as:  $Po = (t_{open}/t_{total})/n$  where 'n' is an estimate of  
500 the number of channels in the membrane patch derived from the maximum number of open levels  
501 observed in the recording. Recordings of 60 s duration ( $t_{total}$ ) at a membrane potential of -80 mV  
502 were analysed by using a 50% threshold technique to define current transitions and calculate  $t_{open}$   
503 to determine Po. Open probability data were obtained from 3 to 10 individual protoplasts (see Figure  
504 S2 and Data S1). To compare different genotypes, the increase in Po in response to ATP and  
505 ATP+14-3-3 was calculated for each experiment and 'fold changes' were subsequently averaged  
506 across experiments. ATP was added as Mg-ATP at a final concentration of 0.5 mM. 14-3-3 protein  
507 (as Hv14-3-3B or Hv14-3-3C; GenBank accessions X93170 and Y14200 respectively [36]) was a  
508 kind gift from Bert de Boer (Vrije Universiteit, Amsterdam) and added to a final concentration of  
509 0.2 µg/ml.

#### 510 **Imaging**

511 Intact and osmotically disrupted guard cells were photographed on a Zeiss epifluorescence  
512 microscope using bright light, DIC or epifluorescence (465-495 nm excitation and 515 nm emission  
513 wavelength) with a 20x, 40x or 63x objective. Confocal imaging was performed using a Zeiss  
514 LSM510 Meta microscope (Carl Zeiss, <http://www.zeiss.com>).

#### 515 **Leaf Stomatal conductance and apertures**

516 To record responses to ABA, leaves of mature plants were removed at approx 10:00h and incubated  
517 in 'opening' buffer (10 mM KCl, 10 mM MES-KOH pH 6.15) for 2 h in the light to induce  
518 maximum opening. Subsequently, H<sub>2</sub>O gas exchange was determined (in the same buffer) using an  
519 infrared gas analyser, Li-Cor 6400 (LI-COR, Cambridge, UK) to obtain a starting conductance  
520 value. Subsequent values were obtained after 30 min incubation in control (no ABA) or ABA (1,  
521 10 or 100 µM final concentration) buffer. Each experiment was carried out using three leaves and  
522 in total 12-24 leaves from 3-4 individual plants were used for each treatment. Changes recorded in  
523 control treatments (no ABA) were subtracted from those obtained from ABA treated leaves.

524 To obtain time courses for the response to elevated [CO<sub>2</sub>], stomatal conductance was measured  
525 using infrared gas analysis. Measurements were performed using a portable photosynthesis system  
526 attached to a leaf chamber with a 2.5 cm<sup>2</sup> leaf area (Walz GFS-3000). CO<sub>2</sub> was scrubbed from

527 external air using soda lime and resupplied from a liquid CO<sub>2</sub> cartridge to maintain CO<sub>2</sub>  
528 concentrations of either 400 or 1000 ppm. Temperature was maintained at 22°C and the absolute  
529 humidity to 16000 ppm to obtain a relative humidity of 64.5%. Air flow was 400 μmol.s<sup>-1</sup>, light  
530 intensity was 120 μmol.m<sup>-2</sup>.s<sup>-1</sup>. For each measurement, an individual mature leaf was placed in the  
531 leaf chamber, while still attached to the plant. Leaves were left in the chamber for 30 min before  
532 measurements were taken to allow them to acclimatise to chamber conditions and for gas exchange  
533 to stabilise. Measurements were then logged every 10 secs and averaged every 2.5 min. Data  
534 represent the mean +-SEM from 3 different plants.

535 To obtain stomatal apertures, leaf epidermes were removed from fully expanded leaves of 5 to 6  
536 week old plants. They were collected cuticle-side up on CO<sub>2</sub>-free 10 mM MES/KOH (pH 6.15) in  
537 5cm Petri dishes (Sterilin, UK) at 22°C for 30min. Epidermal peels were transferred to fresh Petri  
538 dishes and incubated in the light under a fluence rate of 120 μmol.m<sup>-2</sup>.s<sup>-1</sup> in 50mM KCl, 10 mM  
539 MES/KOH (pH 6.15) at 22°C 2 hours whilst being aerated with an air stream containing 400 ppm  
540 [CO<sub>2</sub>] from a pressurised cylinder (BOC, Special Gasses, UK) by bubbling directly into the buffer.  
541 Subsequently, peels were either aerated with 1000ppm [CO<sub>2</sub>] or continued to be aerated with  
542 400ppm [CO<sub>2</sub>]. After 3h, peels were removed, mounted on slides and measurements of stomatal  
543 aperture were recorded using an inverted microscope (Leica DM-IRB, Leica UK). Forty stomatal  
544 pores were measured per treatment in three separate replicated experiments (total stomatal number  
545 = 120; n = 3). To avoid bias, experiments were performed without knowing the identity of the plants  
546 and the treatments until data were collected. Data were analysed using one-way ANOVA.

#### 547 **Immunoblotting**

548 Guard cell protoplast preparations were visually inspected and only used when containing fewer  
549 than 1% mesophyll protoplasts. ABA treatment (40 μM, 1 hour) was either done on intact leaves in  
550 buffer (containing 20 mM KCl, 10 mM MES/KOH pH 6.1) at ~150 μmol.s<sup>-1</sup>.m<sup>-2</sup> light, or on isolated  
551 protoplasts in buffer (containing 500 mM Sorbitol, 10 mM KCl, 1 mM CaCl<sub>2</sub>, 10 mM MES/Tris  
552 pH 5.5). In the latter case, protoplasts were isolated from *tpk1* mutants, and transiently transformed  
553 with pART7:TPK1:YFP [15]. Around 16h after transformation, protoplasts were divided in two  
554 population with one exposed to ABA (conditions as above). After treatment, protoplasts were  
555 resuspended in 'RIPA' buffer (1% Triton X 100, 0.1% SDS, 100 mM NaCl, 10 mM Na<sub>2</sub>HPO<sub>4</sub> and  
556 10 mM NaH<sub>2</sub>PO<sub>4</sub>, pH 7.2 plus protease inhibitor cocktail 'cComplete EDTA free' from Roche UK)  
557 and stored at -20°C.

558 For analysis of phosphorylation levels, protein samples (40 $\mu$ g) were precipitated by methanol-  
559 chloroform extraction, separated by SDS-10% acrylamide gel electrophoresis and transferred onto  
560 nitrocellulose (Hybond-ECL, GE Healthcare). Prior to blocking (5% BSA, TBS), protein levels  
561 were visualised with Ponceau S (0.1% w/v in 1% Acetic acid). TPK1 phosphorylation was detected  
562 by immunoblotting overnight with anti-pBAD-Ser136 (1:200, i.e. 75  $\mu$ L in 15 ml, rabbit polyclonal  
563 serum, Santa Cruz sc-12969; secondary antibody IRDye 800CW Donkey anti-rabbit, LI-COR 926-  
564 32213) and visualised by infrared fluorescence (ODYSSEY CLx, LI-COR). Average  
565 phosphorylation signal was calculated using densitometry (ImageJ v 1.48).

### 566 **Isolation of tonoplasts and Western blotting**

567 Five plants at the rosette stage were coated using a paint brush with tween 0.05%, cycloheximide  
568 (CHX) 50  $\mu$ M or chlorpromazine (CPZ) 50  $\mu$ M in tween 0.05%, one hour before being sprayed  
569 with ABA (100  $\mu$ M) or with a mock solution (tween 0.05%). One hour after ABA treatment, the  
570 samples were frozen in liquid nitrogen and ground using a mortar and a pestle. Microsomes were  
571 extracted according to Lund and Fuglsang [37] with an altered homogenisation buffer according to  
572 Rea, et al. [38]. Briefly, ground material was extracted in 1.1 M glycerol, 5 mM Tris-EDTA, 5 mM  
573 DTT, 1% [w/v] PVP-40, 1 mM PMSF, 70 mM Tris-Mes [pH 8.0] and centrifuged at 6,000g for 10  
574 min. The pellet was resuspended in 3.5 mL buffer 330/5 (0.33 M sucrose, 5 mM potassium  
575 phosphate pH 7.8) using a glass homogenizer. Three grams of microsomal fraction was added on  
576 top of 9 g polymer solution (3.72 g of 20% Dextran T500 solution, 1.86 g of 40% PEG4000 solution,  
577 1.08 g sucrose, 225  $\mu$ L potassium phosphate buffer 0.2 M pH 7.8, 18  $\mu$ L KCl 2 M, H<sub>2</sub>O up to 9 g).  
578 In parallel, a blank tube was made with 3 g of buffer 330/5 that was added on top of the polymer  
579 solution. The tubes were gently inverted 12 times and centrifuged at 1,000g for 5 min. The lower  
580 phase enriched in tonoplast was collected and re-purified using the top phase of the blank tube. The  
581 bottom phase was collected and diluted 10 times with buffer 300/5. The tonoplasts were centrifuged  
582 at 100,000g for 60 min. The lower phase enriched in tonoplast was resuspended in 0.1 ml RIPA  
583 buffer (Fisher scientific, Nottingham, UK) and loaded onto a 4-12% SDS-PAGE NuPAGE™  
584 (Thermofisher, UK). The western blotting was performed according to Pijacka, et al. [32]. Briefly,  
585 an Amersham ECL Plex Western blotting system was used on which the gel was run for 2 hours at  
586 120V and protein was subsequently transferred onto a low-fluorescent PVDF membrane (GE  
587 Healthcare, Buckinghamshire, UK) using NuPAGE Transfer Buffer (Thermofisher, UK) for 1 hour  
588 at 30V in a mini gel tank (Thermofisher, UK). The membrane was cut horizontally in two parts,

589 with the upper part incubated overnight at 4°C with anti-GFP antibody (at 1:2000 dilution) and the  
590 bottom part with anti TIP1-1 antibody (at 1:5000 dilution), ensuring equal protein ratio between  
591 lanes. Fluorescent secondary antibodies were incubated for one hour and the blots were imaged  
592 using fluorescent laser scanner (Typhoon, GE Healthcare, Buckinghamshire, UK). Quantification  
593 of bands was performed using CLIQS software (Totallab, Newcastle upon Tyne, UK).

594 To determine change in tonoplast expression in response to ABA or CO<sub>2</sub>, plants were treated for up  
595 to 2h with 50 μM ABA or 1000 ppm CO<sub>2</sub>. Immunoblotting was carried out as described above and  
596 relative expression levels were determined using TIP1;1 as marker and ImageJ [31] software to  
597 quantify band intensities.

#### 598 **QUANTIFICATION AND STATISTICAL ANALYSIS**

599 Where statistical testing of data was applied, it is indicated in the legend of the respective figure, as  
600 is the number ('n') of experimental replicates. For ANOVA analyses, Prism 6 (Graphpad software)  
601 was used. If ANOVA revealed significant ( $p < 0.05$ ) effect of group, post hoc test used to determine  
602 p values for all relevant comparisons is mentioned in the figure legends.

603 **Data S1 'Patch clamp open probabilities' (related to Figures 1E and S2A).** The spreadsheet  
604 shows open probabilities for each kinase genotype in control, plus ATP or plus ATP+14-3-3  
605 conditions.

606

607

608

609

610

611

612

613

614

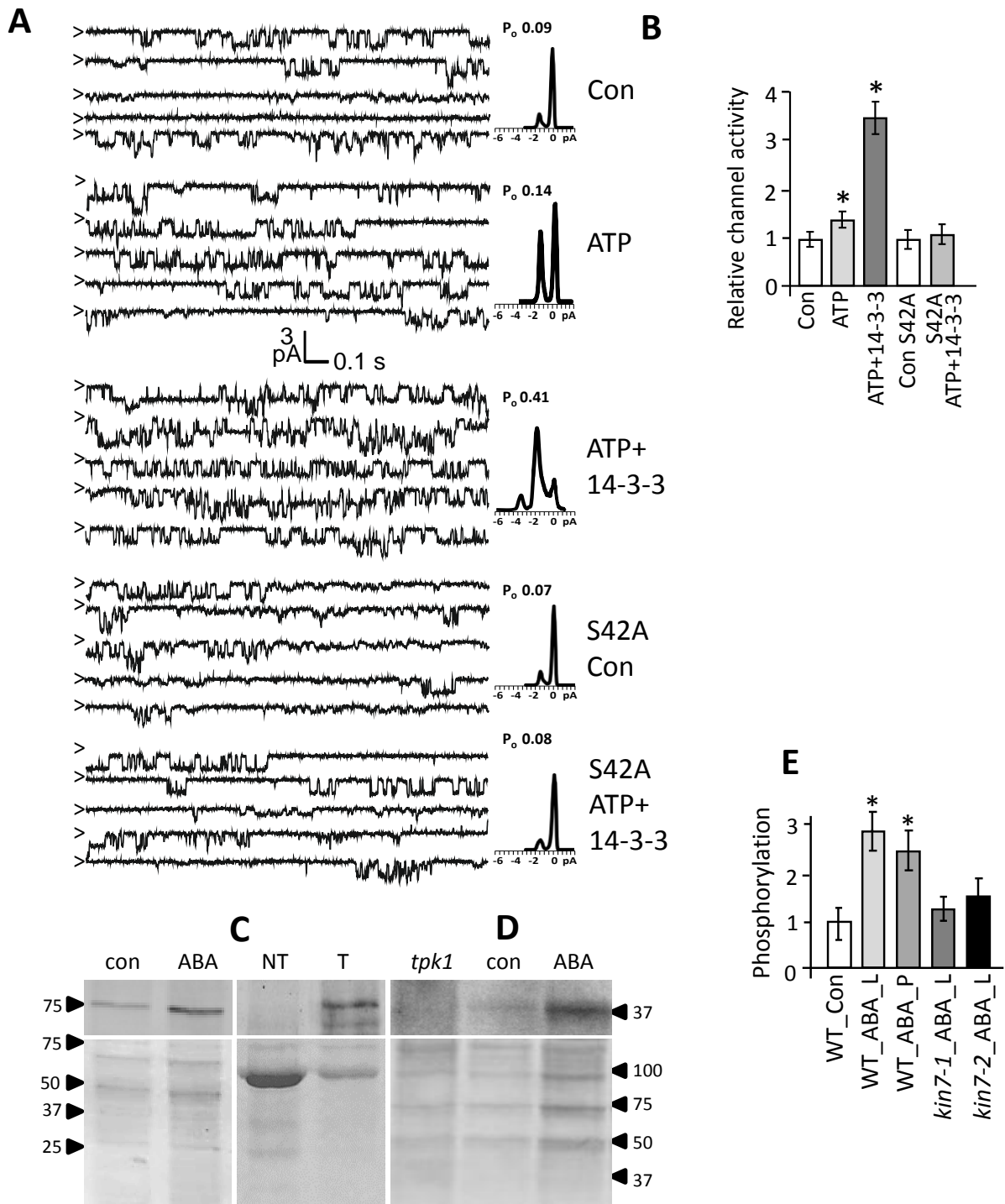
615

616

617

618

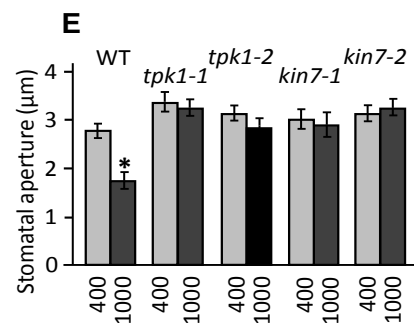
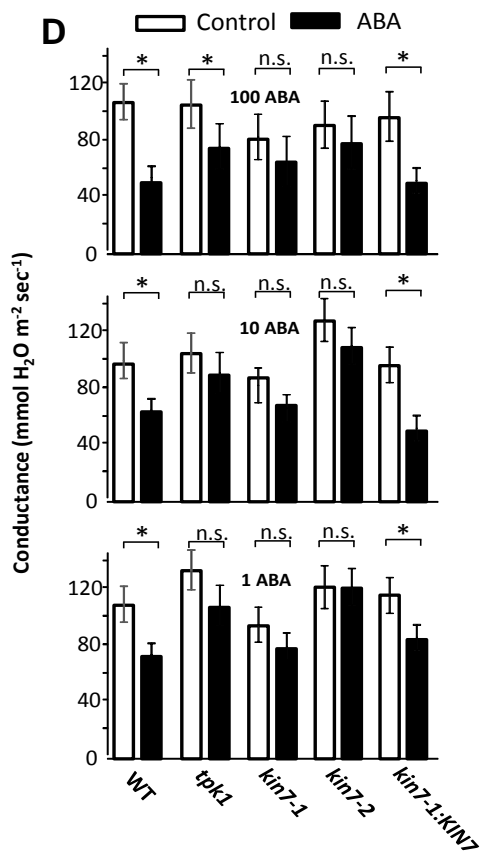
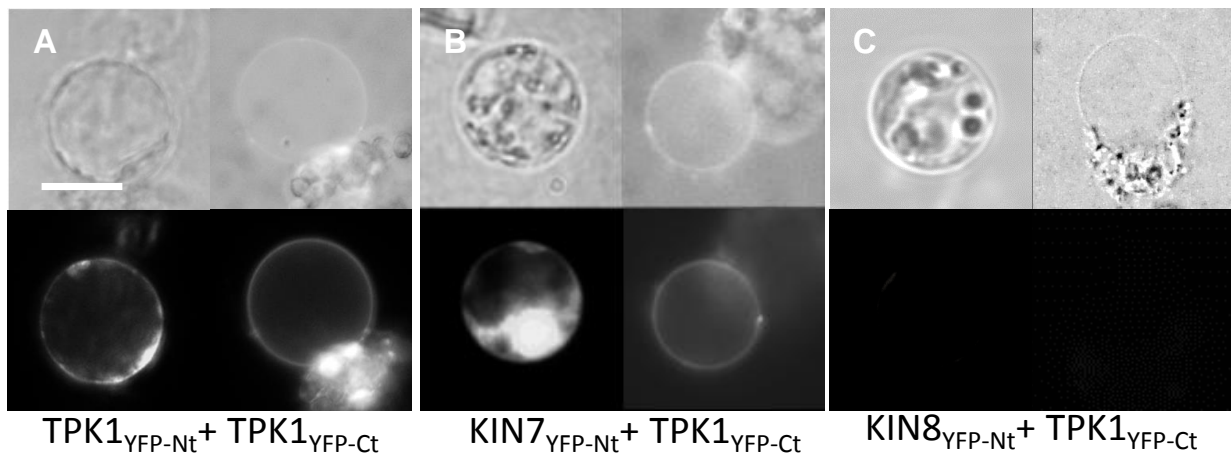
619



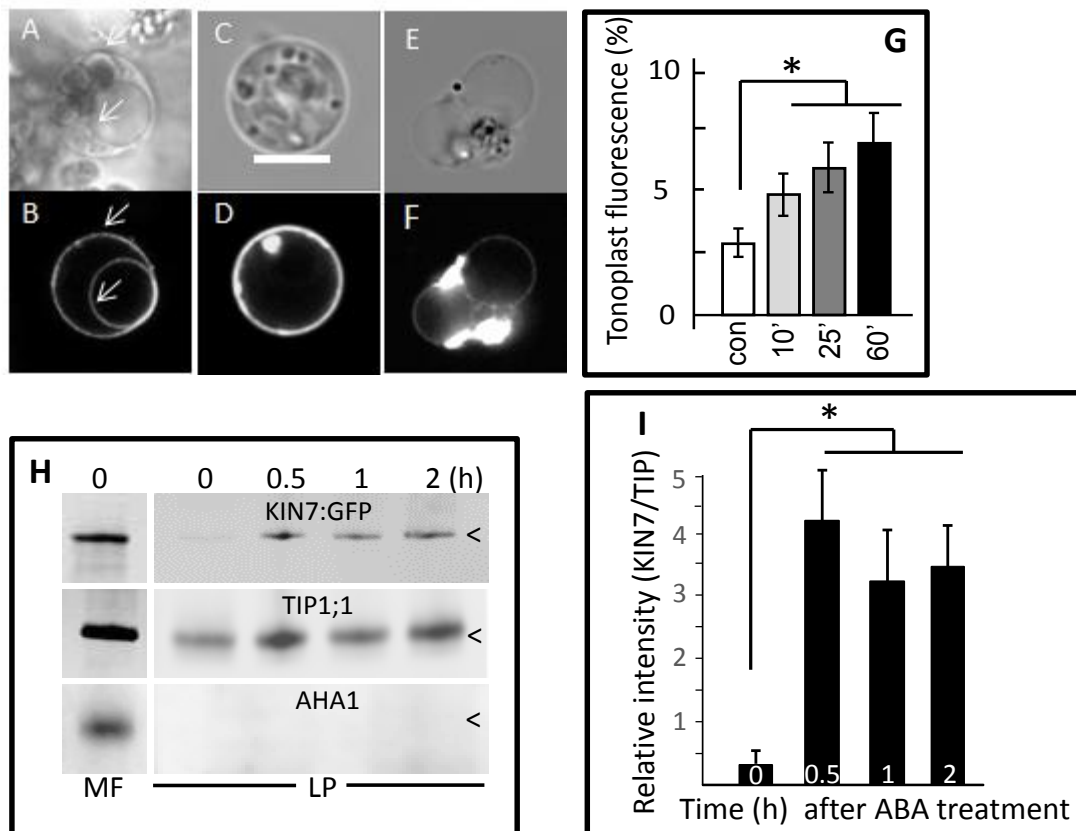
620  
621  
622  
623  
624  
625

Fig 1



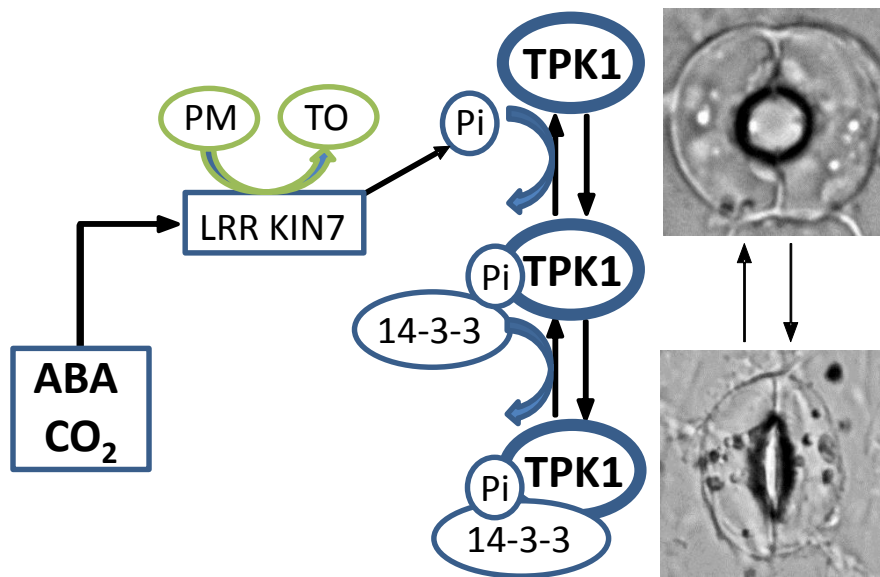


626  
 627  
 628 Fig 2  
 629  
 630  
 631  
 632



633  
 634  
 635  
 636  
 637  
 638  
 639  
 640  
 641  
 642  
 643  
 644  
 645  
 646  
 647  
 648

Fig 3



649  
 650  
 651  
 652  
 653  
 654  
 655  
 656  
 657  
 658  
 659  
 660  
 661  
 662  
 663  
 664  
 665  
 666  
 667  
 668  
 669

Fig 4

27

670

671